ТРАНСПОРТНЫЕ СВОЙСТВА ДВУХКОМПОНЕНТНЫХ РАДИЕВО-ГАЛОГЕННЫХ РАЗРЕЖЕННЫХ ГАЗОВЫХ СРЕД

Д. Н. МЕНЯЙЛОВА[1], М. Б. ШУНДАЛОВ[1, 2], Ю.-Ч. ХАНЬ[2, 3]

[1]Белорусский государственный университет, пр. Независимости, 4, 220030, г. Минск, Беларусь
[2]Совместный институт Даляньского политехнического университета
и Белорусского государственного университета, 116024, г. Далянь, Китай
[3]Даляньский политехнический университет, 116024, г. Далянь, Китай

Использованы неэмпирические функции потенциальной энергии и классической кинетической теории. В зависимости от температуры газовой смеси (вплоть до 3000 К) рассчитаны некоторые транспортные свойства (коэффициенты диффузии, вязкости и теплопроводности) двухкомпонентных разреженных газовых сред, состоящих из атомов радия и атомов галогена (F, Cl, Br, I). Расчеты выполнены на основе последовательного аналитического и (или) численного вычисления интегралов для угла рассеяния, сечения рассеяния и столкновений. Разработана подробная методика расчета транспортных свойств с использованием потенциала Морзе. Рассмотрены некоторые численные трудности, возникающие из-за особенностей подынтегральных выражений и разрывного характера переменной интегрирования. Показана зависимость транспортных свойств от массы изотопа. Оценены возможные ошибки, вносимые применением модельной потенциальной функции Морзе вместо реального потенциала взаимодействия между атомами. Полученные результаты могут быть использованы при планировании экспериментов по прямому лазерному охлаждению моногалогенидов щелочноземельных металлов.

Ключевые слова: транспортные свойства; интегралы столкновений; моногалогениды радия; лазерное охлаждение.

Авторы:
Дарья Николаевна Меняйлова – старший преподаватель кафедры высшей математики и математической физики физического факультета.

Максим Борисович Шундалов – кандидат физико-математических наук, доцент; доцент кафедры физической оптики и прикладной информатики физического факультета[1], доцент[2].

Юн-Чан Хань – доктор физико-математических наук; профессор[2], профессор физического факультета[3].

Authors:
Darya N. Meniailava, senior lecturer at the department of high mathematics and mathematical physics, faculty of physics.
meniailava@bsu.by
https://orcid.org/0000-0002-8848-8447

Maksim B. Shundalau, PhD (physics and mathematics), docent; associate professor at the department of physical optics and applied informatics, faculty of physics[a], and associate professor[b].
shundalau@bsu.by
https://orcid.org/0000-0002-2911-7101

Yong-Chang Han, doctor of science (physics and mathematics); professor[b] and professor at the department of physics[c].
ychan@dlut.edu.cn

TRANSPORT PROPERTIES OF TWO-COMPONENT RADIUM − HALOGEN DILUTE GAS MEDIA

D. N. MENIAILAVA[a], *M. B. SHUNDALAU*[a, b], *Y.-C. HAN*[b, c]

[a]*Belarusian State University, 4 Niezaliežnasci Avenue, Minsk 220030, Belarus*
[b]*Joint Institute of the Dalian University of Technology and Belarusian State University, Dalian 116024, China*
[c]*Dalian University of Technology, Dalian 116024, China*
Corresponding author: D. N. Meniailava (meniailava@bsu.by)

Based on state-of-the-art *ab initio* potential energy functions and classical kinetic theory, some transport properties (diffusion, viscosity and thermal conductivity coefficients) of two-component dilute gas media of radium and halogen (F, Cl, Br, I) atoms were predicted as functions of the translation temperature up to 3000 K. Calculations were performed by sequential analytical and (or) numerical computations of deflection angle, cross-section and collision integrals. A detailed methodology for the calculation of the transport properties using the Morse potential was developed. Some numerical difficulties arising due to the singularity of the integrands and discontinuous character of the variable of integration are considered. The dependence of transport properties on isotope mass is also shown. Possible errors introduced by using the model Morse potential function instead of the real potential for the interaction between atoms are estimated. These data can be useful for the planning of the experiments on the direct laser cooling of the monohalides of alkaline earth metals.

Keywords: transport properties; collision integrals; radium monohalides; laser cooling.

Introduction

Laser cooling is one of the effective techniques to obtain ultracold molecules [1; 2]. Among possible applications of ultracold molecules, such as the creation of a Bose – Einstein condensate, quantum information processing, controlled chemical reactions, a new promising application of ultracold molecules containing heavy nuclei, namely, research for electron's electric dipole moment, was recently proposed [3].

The monohalides of alkaline earth metals are promising diatomic molecules for the direct laser cooling due to the coincidence of the equilibrium internuclear distances of potential energy curves (PECs) involved in the cooling scheme states and, as a consequence, highly diagonal Franck – Condon factors. Other essential features required for effective direct laser cooling are strong transition dipole moment between the states involved in the cooling scheme and the absence of intervening electronic states between them in order to avoid leaks in the cooling cycle [2]. Generally, the monohalides of alkaline earth metals possess the mentioned key factors. Recently, the strontium monofluoride (SrF) [4−6] and calcium monofluoride (CaF) [7–9] molecules were successfully cooled and caught into a magneto-optical trap.

Among all monohalides of alkaline earth metals, the radium ones are least studied, possibly due to the high radioactivity of the radium. Nevertheless, the radium monofluoride (RaF) molecule is considered the most promising candidate for direct laser cooling in order to use it for measuring molecular parity violation [10]. In the recent experimental studies [11; 12] numerous molecular spectroscopic parameters for the lowest states of the RaF molecule with different radium isotopes were obtained for the first time. The method used in [11; 12] provides breakthrough possibilities for the high-precision studying short-lived radioactive molecules, including the development of laser cooling schemes. The latter task has different sides. On the one hand, it is necessary to calculate at the high level of theory the PECs involved in the cooling scheme states, spectroscopic and radiative characteristics of the vibronic states, etc. Another aspect of the problem under consideration is the calculation of the transport properties of alkaline earth metal atoms and halogen atoms under conditions of dilute gaseous media at various particle concentrations and temperatures. These data can be useful for the planning of the experiments. The most important transport properties that determine the dynamics of pair collisions in a gas medium are the coefficients of viscosity (pure gases and mixtures), thermal conductivity, diffusion, and effective collision cross-sections [13].

Lately, we performed the state-of-the-art FS-RCCSD (Fock-space relativistic coupled cluster singles and doubles) [14] calculations for the RaF [15], RaBr [16], and RaI [17] molecules. The results of these studies show that radium monohalides can be used for direct laser cooling. In this study, we use the classical Chapman – Enskog kinetic theory [13] in order to predict the transport properties of the dilute radium – halogen gas

media. The transport properties are evaluated in the terms of reduced collision integrals, and some numerical difficulties arise due to the singularity of the integrands and discontinuous character of the variable of integration [18; 19].

The main goals of the work are to develop a consistent scheme for the calculation of transport properties of the dilute gas media based on the classical kinetic theory [13] and Taylor's algorithm [18] and to evaluate some transport properties of the dilute radium – halogen media based on the Morse potential function for the interaction between atoms and modern possibilities of the numerical methods.

Theoretical details

It is convenient to consider the problem of two colliding particles with masses m_1 and m_2 in the center-of-mass system. In other words, the above-mentioned three-dimension problem turns into the two-dimension one for the motion of only one particle with reduced mass $\mu = \dfrac{m_1 m_2}{m_1 + m_2}$ in the spherically symmetric potential field $\Phi(r)$. In this case, the collision process can be characterised by the following parameters: the total energy of particles E, which is equal to their relative initial kinetic energy $E = \dfrac{1}{2}\mu v_\infty^2$; the deflection angle χ; the impact parameter b (fig. 1). According to definition of the deflection angle, its value varies from 0 to π, excluding the orbiting case (see below). The value of π corresponds to the situation of head-on collision with zero impact parameter, and the value of 0 corresponds to the situation with avoiding collision at very large values of b.
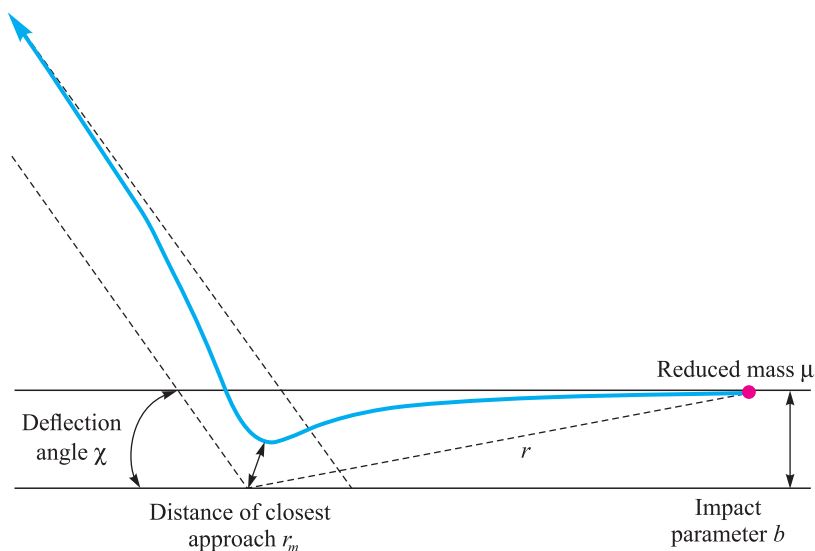

Fig. 1. The two particles collision in the center-of-mass system

Moreover, the two-dimension colliding problem can be reduced to the one-dimension one for the motion of the particle with reduced mass μ in some effective potential field $\Phi_{eff}(r)$, which is given by the following equation:

$$\Phi_{eff}(r) = \Phi(r) + E\frac{b^2}{r^2}. \tag{1}$$

According to the classical kinetic theory of gases [13], the diffusion coefficient D, the viscosity coefficient η and the thermal conductivity coefficient λ for low-density atomic gases at the first approximation are

$$D = \frac{\sqrt[3]{\dfrac{\pi k_B^3 T^3}{2\mu}}}{8\pi\sigma^2 \Omega^{(1,1)}(T^*)}, \tag{2}$$

$$\eta = \frac{\sqrt[5]{2\mu\pi k_B T}}{6\pi\sigma^2 \Omega^{(2,2)}(T^*)}, \tag{3}$$

$$\lambda = \frac{\sqrt[25]{\dfrac{\pi k_B T}{2\mu}}}{32\pi\sigma^2 \Omega^{(2,\,2)}\left(T^*\right)},\tag{4}$$

where k_B is the Boltzmann constant; σ is the collision diameter, its value is equal to the distance between particles, for which $\Phi(r) = 0$; $\Omega^{(1,\,1)}\left(T^*\right)$ and $\Omega^{(2,\,2)}\left(T^*\right)$ are reduced collision integrals as functions of the reduced temperature $T^* = \dfrac{k_B T}{\varepsilon}$; ε is a parameter having the dimension of energy, its value is chosen as dissociation energy D_e for the potential energy function $\Phi(r)$ of interacting particles.

The collision integrals $\Omega^{(l,\,s)}\left(T^*\right)$ are expressed in the terms of cross-section integrals $Q^{(l)}(E)$:

$$\Omega^{(l,\,s)}\left(T^*\right) = \frac{1}{(s+1)!\,T^{s+1}} \int_0^\infty e^{-\frac{E}{T}} E^{s+1} Q^{(l)}(E)\,dE.\tag{5}$$

In its turn, the cross-section integrals $Q^{(l)}(E)$ are

$$Q^{(l)}(E) = \frac{2}{1 - \dfrac{1 + (-1)^l}{2(1+l)}} \int_0^\infty \left(1 - \cos^l \chi\right) b\,db.\tag{6}$$

The integral for the deflection angle $\chi(E,\,b)$ is determined as follows:

$$\chi(E,\,b) = \pi - 2b \int_{r_m}^\infty \frac{dr}{r^2 F(r)},\tag{7}$$

where r_m is the distance of closest approach, the function $F(r)$ is

$$F(r) = \sqrt{1 - \frac{\Phi(r)}{E} - \frac{b^2}{r^2}}.\tag{8}$$

The distances b, r and r_m are expressed in the units of the collision diameter σ, while the energies E and $\Phi(r)$ are expressed in the units of the parameter ε.

For the given energy the impact parameter b and the distance of the closest approach r_m are related according to formula (8), where $F(r_m) = 0$, or

$$E r_m^2 - \Phi(r_m) r_m^2 - b^2 E = 0.\tag{9}$$

The last equation should be solved numerically. As a result, the dependence of the distance of closest approach r_m on relative kinetic energy E and impact parameter b can be obtained. The function $r_m(E,\,b)$ allows to calculate integral (7) and to find the dependence of the deflection angle χ on the same parameters.

From the other hand, the equation (9) provides the relationship between b and r_m for a fixed energy:

$$b = r_m \sqrt{\frac{E - \Phi(r_m)}{E}}.\tag{10}$$

The minimal r_m value can be found using the condition $b = 0$, which corresponds to the head-on collision. In this case the equation (9) is reduced to

$$E = \Phi(r_m),\tag{11}$$

and the solution of the equation (11) is denoted as r_E.

Generally, the dependence of the distance of closest approach r_m on b and E has non-trivial character. Figure 2 shows the effective potential energy function $\Phi_{eff}(r)$, evaluated by formula (1), for a fixed energy and for three different values of the impact parameter. The difference between E and Φ_{eff} results in the relative kinetic energy for a given point:

$$E - \Phi_{eff}(r,\,b) = E_k = \frac{1}{2}\mu v^2,\tag{12}$$
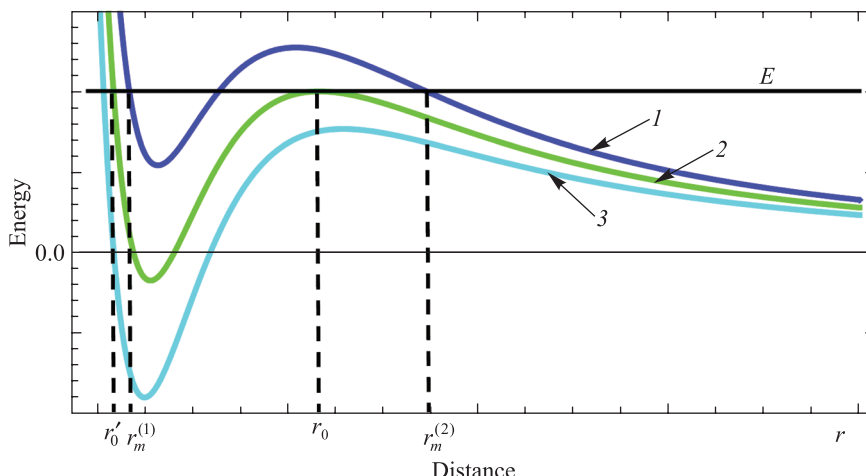
where v is relative radial velocity.

Fig. 2. Effective potential energy function:
the oblique collision (*1*), the orbiting effect (*2*), the head-on collision (*3*)

If the left side of the equation (12) is equal to zero:

$$E - \Phi_{eff}(r, b) = 0, \tag{13}$$

it corresponds to the turning point ($v = 0$) or to the distance of closest approach r_m.

One can see that for some impact parameter $b = b_0$ the condition (13) is satisfied at the point $r = r_0$ (see fig. 2, curve *2*). The second solution of the equation (13) for the case $b = b_0$ lies in the region $r < r_0$ and is denoted as r_0'. For the case $b > b_0$ (see fig. 2, curve *1*) there are also two values for the distance of closest approach r_m, namely $r_m^{(1)} < r_0$ and $r_m^{(2)} < r_0$. The only last one has physical meaning since a particle cannot penetrate to the region $r < r_0$. For the case $b < b_0$ (see fig. 2, curve *3*) the equation (13) has only one solution, and its value $r_m < r_0'$.

To find the r_0 value, it is necessary to consider the joint solution of the equation (13) and the extremum condition (14):

$$\frac{d\Phi_{eff}}{dr} = 0. \tag{14}$$

Elimination of the impact parameter b for the system (13), (14) gives equation

$$2(E - \Phi) - r\frac{d\Phi}{dr} = 0, \tag{15}$$

which can be solved numerically for r_0. The r_0' is a smaller root of the equation (13).

So, for $b > b_0$ the distance of closest approach is greater than r_0, and for $b < b_0$ the distance of closest approach is less than r_0'. It means that the distance of closest approach as a function of the impact parameter is discontinuous for $b = b_0$, and distances of closest approach in the interval $r_0' < r_m < r_0$ are physically impossible.

From the physical point of view, values $b > b_0$ correspond to rather oblique collisions, for which deflection of particles occurs with fairly small angles, and attractive forces between particles dominate over repulsive ones. Case $b < b_0$ corresponds to almost head-on collisions, deflection occurs with large angles, and repulsive forces play main role. Case $b = b_0$ is characterised by the orbiting effect, or the formation of quasi-bound state of two particles. In this case particles long time orbit each other at a distance r_0.

The critical energy E_c, for which the orbiting occurs and below which r_m has discontinuous character, can be found according to following. Based on equation (15) one can obtain the expression for energy:

$$E = \frac{1}{2}r_0\frac{d\Phi}{dr_0} + \Phi(r_0). \tag{16}$$

Extremum of the energy corresponds to the critical energy E_c:

$$\frac{dE}{dr_0} = \frac{1}{2}\left(3\frac{d\Phi}{dr_0} + r_0\frac{d^2\Phi}{dr_0^2}\right) = 0. \tag{17}$$

So, the solution of the equation (17) gives value of the critical distance of closest approach r_c. Substitution of the r_c into the equation (16) gives the critical energy E_c.

Thus, for the calculation of the deflection angle χ for energies $E < E_c$ the integral (7) should be divided into two parts: the integral over $r_E(E)$ to $r_0'(E)$ and the integral over $r_0(E)$ to infinity. For energies $E > E_c$ the integral (7) is over $r_E(E)$ to infinity.

Since the orbiting effect corresponds to the formation of a quasi-bound state of interacting particles, they orbit each other like a bound system. Therefore, the deflection angle increases continuously, and its value tends to infinity (fig. 3).
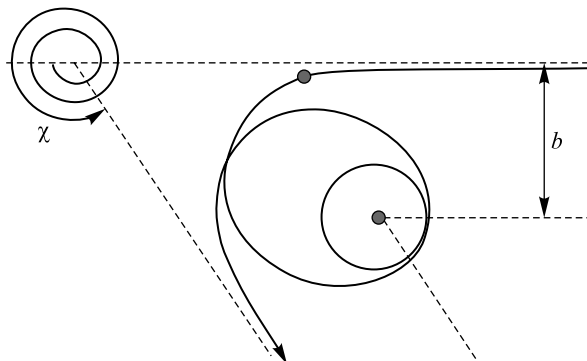

Fig. 3. The two particles collision in the orbiting case at energies less
than E_c, where the deflection angle χ varies from zero to infinity

Figure 4 represents the dependence of the $(1 - \cos\chi)$ function on the impact parameter b for several values of reduced energy E. Figure 4, *a*, corresponds to relative energy $E = 0.014$, which is less than the critical energy ($E_c = 0.284$), and, therefore, it demonstrates the orbiting effect. In addition, figure 4, *b*, represents energy $E = 0.324$ near-critical one, and $(1 - \cos\chi)$ function rapidly oscillates between values zero and two. Figure 4, *c* and *d*, correspond to energy values, which are greater ($E = 0.490$) or much greater ($E = 42.0$) than critical energy. The latter one demonstrates monotonic dependence of the $(1 - \cos\chi)$ function on the impact parameter b.

The exact empirical potentials for interaction between radium atom and halogen atoms (F, Cl, Br and I) are unknown. In order to calculate the required transport properties, we have used the *ab initio* PECs for the ground state of the RaF [15], RaCl [20], RaBr [16] and RaI [17] molecules. These PECs have been calculated at the FS-RCCSD [14] level of theory, which is one of the most successful tools for predicting the electronic structure and properties of molecular compounds containing heavy atoms. It provides the most accurate data on PECs and other characteristics of complex molecular systems [15; 20].

The ground state PECs were calculated near their minima and were extrapolated to the larger internuclear distance via the Morse potential [21]:

$$\Phi(r) = D_e \left(1 - e^{-a(r - r_e)}\right)^2 - D_e, \tag{18}$$

where D_e is the dissociation energy; r_e is the equilibrium internuclear distance; a depends on PEC's parameters:

$$a = \frac{\omega_e}{2\pi} \sqrt{\frac{\mu}{2D_e}},$$

where ω_e is a harmonic frequency.

Besides, the ground state PECs, obtained by formula (18), for the radium monohalides are shown in fig. 5. Since the real PEC can significantly differ on the Morse potential function, for comparison we have also calculated the transport properties for the potassium – rubidium medium. In contrast to radium monohalides, the ground state PEC for the KRb molecule has been obtained through both experimental [22] and theoretical [23; 24] methods. We have performed the calculations of the transport properties for the K – Rb medium using exact empirical potential [22] and the model Morse potential. It allows us to estimate possible errors introduced by using the model potential function instead of the real one.

The transport properties as well as the Morse potential, depend on the reduced mass of interacting particles. The radium does not have stable isotopes. The longest-lived isotope of radium is ^{226}Ra with a half-life of about 1600 years. The fluorine has only one stable isotope, namely ^{19}F. The chlorine has two stable isotopes (^{35}Cl and ^{37}Cl) with abundances of 75.77 and 24.23 %, respectively. The bromine also has two stable isotopes (^{79}Br and ^{81}Br) with abundances of 50.69 and 49.31 %, respectively. The iodine has only one stable isotope, namely ^{127}I. The potassium has two stable isotopes (^{39}K and ^{41}K) with abundances of 93.26 and 6.73 %, respectively. The rubidium has only one stable isotope (^{85}Rb) and one long-lived isotope (^{87}Rb) with abundances of 72.17 and 27.83 %, respectively. We calculated the transport properties for the ^{226}Ra – ^{19}F, ^{226}Ra – ^{35}Cl, ^{226}Ra – ^{37}Cl, ^{226}Ra – ^{79}Br, ^{226}Ra – ^{127}I and ^{39}K – ^{85}Rb dilute gas media.
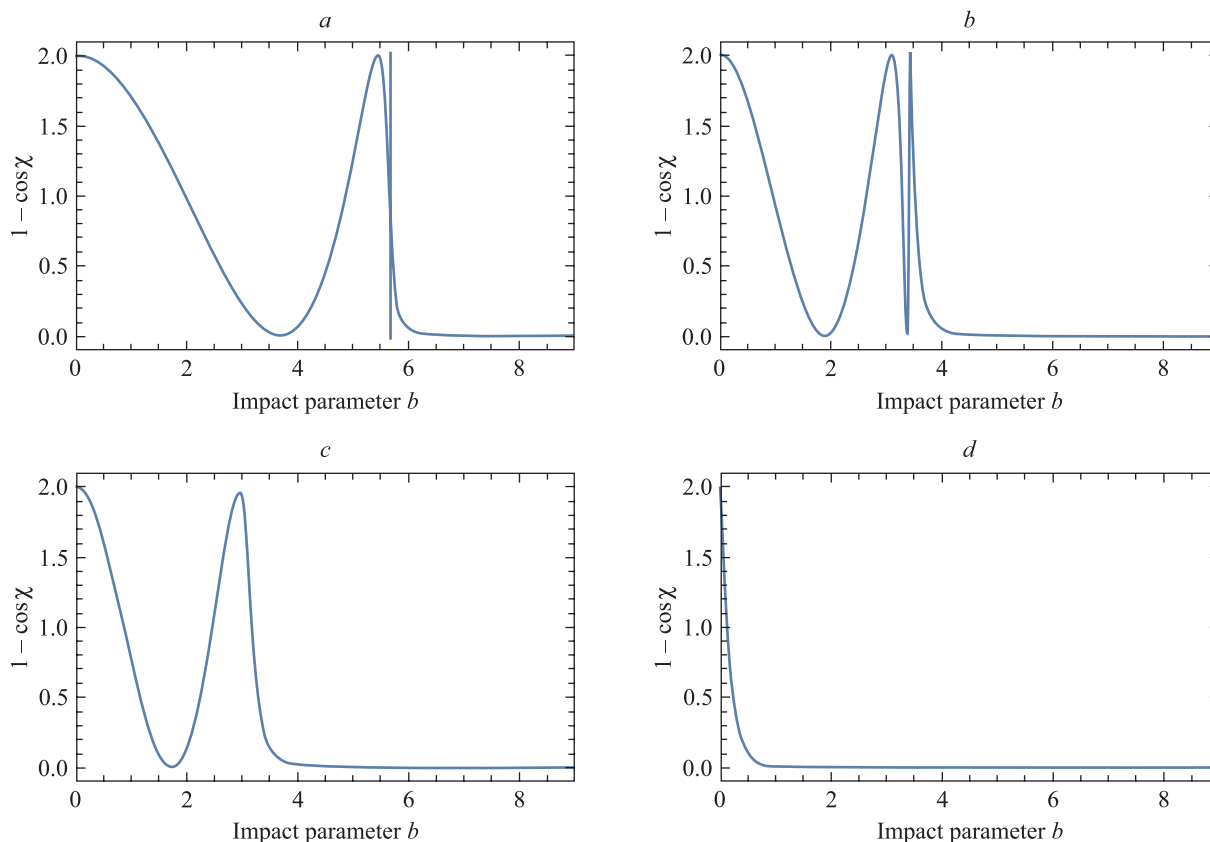
Fig. 4. The dependence of the $(1 - \cos\chi)$ function on the impact parameter b
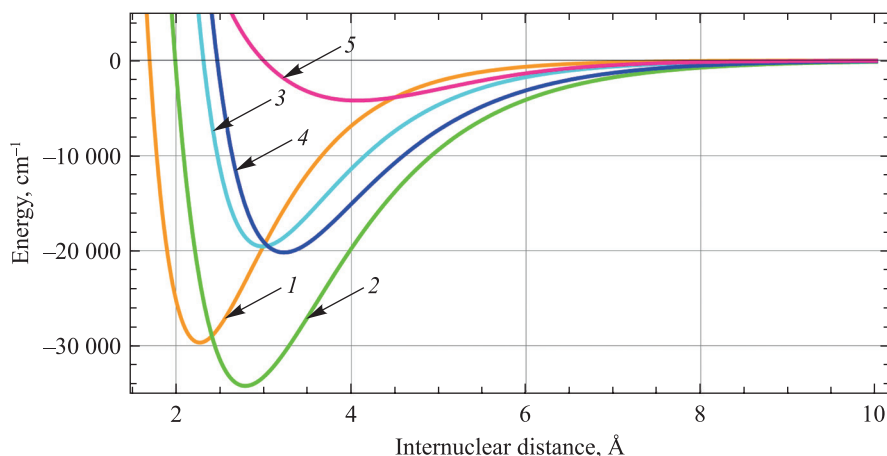for $E = 0.014$ (*a*), 0.324 (*b*), 0.490 (*c*) and 42.0 (*d*)

Fig. 5. Potential energy curves of the ground state
of the RaF (*1*), RaCl (*2*), RaBr (*3*), RaI (*4*) and KRb (*5*) molecules

Calculation details

All calculations were performed in relative units described in the previous section using the package *Wolfram Mathematica* [25]. At the first stage of calculations, a critical distance r_c and critical energy E_c were determined according to formulas (16) and (17). Optimal steps in selected ranges for energies E and impact parameter b were defined.

In the energy range $E < E_c$ the values of r_0 and b_0 were evaluated by using formulas (15) and (10), respectively. The angle χ was calculated for the given energies for the values of b belonging to five different intervals:

I, II, III, IV and V (fig. 6). To calculate the deflection angles using (7) in the intervals I and IV one needs the distances of closest approach r_m to be numerically evaluated using (13) according to the approach described previously. For $b < b_0$, the smallest positive root lying near distance where $\Phi(r) = 0$ was chosen as a solution. For $b > b_0$, the largest positive solution of equation (13), being usually located to the right of the potential inflection point, was taken as r_m. In intervals II and III near the point $b = b_0$, where the orbiting occurs, the angle χ tends to negative infinity. Taking into account this asymptotic behaviour, the angle χ was found as a function

$\sqrt{\dfrac{-c}{b^2 - b_0^2}}$ in interval II to the left of the critical point and as a function $\sqrt{\dfrac{c'}{b^2 - b_0^2}}$ in interval III to the right of

$b = b_0$, where c and c' are positive coefficients determined for each value of E. In the interval V the angle χ takes negative values, slowly increasing tending to zero as b approaches infinity. Considering this tendency, a function of the form $\dfrac{C_6}{b^6} + \dfrac{C_8}{b^8} + \dfrac{C_{12}}{b^{12}}$ was used as function $\chi(b)$, where C_6, C_8 and C_{12} are coefficients determined

for each value of E.

For energies $E > E_c$, the integrals for deflection angles χ were calculated numerically exactly by using formula (7) after evaluating r_m according to (13). As for each value of E deflection angles $\chi(b) \xrightarrow[b \to +\infty]{} 0$ and are negative in the asymptotic region, so for curve-fitting was used the same function as for interval V ($E < E_c$). For energies E slightly larger than E_c in the vicinity of the minimum of the angle χ, where the function changes very rapidly, a more frequent step of b was used to obtain more points for the further interpolation. For the interpolation of the calculated χ points Hermite polynomials of third order were used.
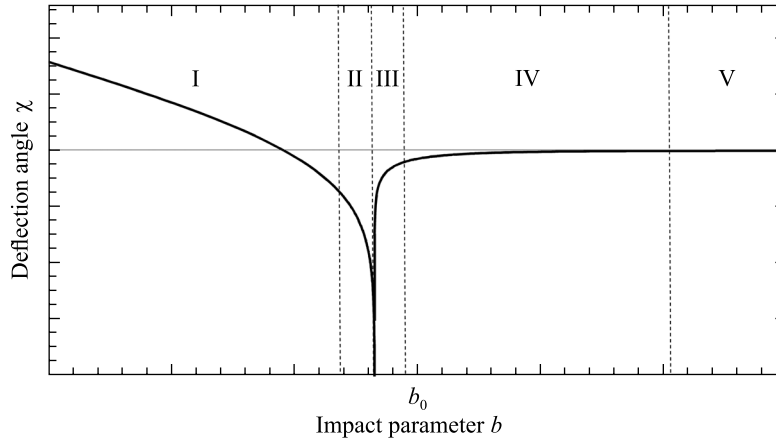

Fig. 6. The dependence of deflection angle χ
on impact parameter b: I–V are intervals

The integrals $Q^{(l)}(E)$ for the scattering cross-sections were calculated according to (6) for $l = 1$ and $l = 2$. For energies $E < E_c$ the values of $Q^{(l)}(E)$ were calculated as $Q^{(l)} = Q_{\mathrm{I}}^{(l)} + Q_{\mathrm{II}}^{(l)} + Q_{\mathrm{III}}^{(l)} + Q_{\mathrm{IV}}^{(l)} + Q_{\mathrm{V}}^{(l)}$, where $Q_i^{(l)}$, $i = \overline{1,\,5}$, are integrals over b belonging to intervals I–V. Integrals $Q_{\mathrm{I}}^{(l)}$, $Q_{\mathrm{IV}}^{(l)}$ and $Q_{\mathrm{V}}^{(l)}$ were calculated numerically, integrals $Q_{\mathrm{II}}^{(l)}$ and $Q_{\mathrm{III}}^{(l)}$ were evaluated analytically. For energies $E > E_c$ the values of $Q^{(l)}(E)$ were obtained as sum of two integrals over b in the intervals of numerically and analytically defined χ data.

Besides, the $Q^{(l)}(E)$ function values for all energies were interpolated by Hermite 3${}^{\mathrm{rd}}$ order interpolation method. To describe the scattering cross sections $Q^{(l)}(E)$ in the regions $E \to 0$ and $E \to +\infty$ the curve-fitting functions of the form of $A^{(l)} E^{p^{(l)}} e^{-k^{(l)} E}$ were applied with the coefficients $A^{(l)}$, $p^{(l)}$ ($p^{(l)} > 0$) and $k^{(l)}$ being defined separately for the discussing regions for different values of l.

The collision integrals $\Omega^{(l,s)}$ were calculated by substituting the obtained integrals for the scattering cross-sections $Q^{(l)}(E)$ into (5) for $l = \overline{1,\,2}$. The range of relative temperatures T^* for these integrals was chosen to correspond to the real temperatures T from 5 to 3000 K for each of the gaseous media under study. As $Q^{(1)}(E)$

and $Q^{(2)}(E)$ were obtained for three ranges of energy: $E \to 0$, values E, selected for the numerical calculation and $E \to +\infty$, than $\Omega^{(l,\,s)}$ were evaluated as sum of three integrals over E. The integrals over second range were obtained numerically. The rest integrals in the sum were calculated analytically as integrals of gamma functions.

The described calculation technique was tested on the Lennard-Jones potential. The integrals calculated by us occurred to be in full agreement with the already known $\Omega^{(l,\,s)}$ collision integrals [13], being widely used for predicting transport properties of gases.

All calculations were performed at a pressure of 1 atm.

Results and discussion

The calculated transport properties for the two-component radium – halogen dilute gas media as functions of the translation temperature in the range 5–3000 K are shown in fig. 7, *a*, 8, *a*, and 9, *a*. The dependencies of the transport properties on chlorine isotope mass are presented in fig. 7, *b*, 8, *b*, and 9, *b*, where inserts demonstrate mentioned functions for high temperatures. Figures 7, *c*, 8, *c*, and 9, *c*, show calculated transport properties for the K – Rb medium using exact empirical (curve *8*) and model Morse (curve *7*) PECs.

The difference in behaviour of the diffusion D and thermal conductivity λ functions and viscosity η function is due to the following reasons. The dependencies of the D, λ and η coefficients on medium's characteristics are (see also equations (2)–(4))

$$D \sim \frac{\sqrt[T]{\dfrac{T}{\mu}}}{\Omega^{(1,\,1)}}, \tag{19}$$

$$\lambda \sim \frac{\sqrt{\dfrac{T}{\mu}}}{\Omega^{(2,\,2)}}, \tag{20}$$

$$\eta \sim \frac{\sqrt[\mu]{\dfrac{T}{\mu}}}{\Omega^{(2,\,2)}}. \tag{21}$$

Since the dependencies of the collision integrals $\Omega^{(1,\,1)}$ and $\Omega^{(2,\,2)}$ on temperature have the same character, namely, they monotonically decrease when temperature increases, the reduced mass and the PEC's parameters are crucial in differences of the coefficients for different media. For the diffusion coefficient D (see fig. 7, *a*) and thermal conductivity coefficient λ (see fig. 8, *a*) for the Ra – Cl and Ra – Br media mentioned dependencies partly compensate each other (see also fig. 5). As a result, D and λ functions for the Ra – Cl and Ra – Br media are similar. The diffusion coefficient D (19), in fact, differs from the thermal conductivity coefficient λ (20) only by a factor of temperature, which results in a faster rise of corresponding dependencies for high temperature. Wherein, a character of rising of the functions remains the same.

Generally, the transport properties are weakly dependent on isotope mass (see fig. 7, *b*, 8, *b*, and 9, *b*). For low temperatures, this dependence almost vanishes at all.

The viscosity coefficient η (21), in fact, is the thermal conductivity coefficient λ (20), which is multiplied by the reduced mass μ. As a result, a character of rising of the η function drastically differs on λ function (comp. fig. 8, *a*, and 9, *a*). It is reflected in dependencies of the thermal conductivity coefficient λ and viscosity coefficient η for the Ra – Cl medium for different chlorine isotopes (see fig. 8, *b*, and 9, *b*). The thermal conductivity coefficient λ function for the chlorine-35 isotope lies above the chlorine-37 one, wherein for the viscosity coefficient η the dependencies are reversed.

However, the analysis of dependencies of the transport properties on temperature for the K – Rb medium (see fig. 7, *c*, 8, *c*, and 9, *c*) shows that the model Morse potential energy function underestimates the D, λ and η coefficients compared with exact empirical one [22]. Our results are in agreement with calculations of [26] on the alkali metal (Rb, Cs) – rare gas (He, Ne, Ar, Kr, Xe) media, for which calculated transport properties using the Morse potential are also underestimated relatively experimental values. It should be taken into account when comparing theoretical results with future experimental data.
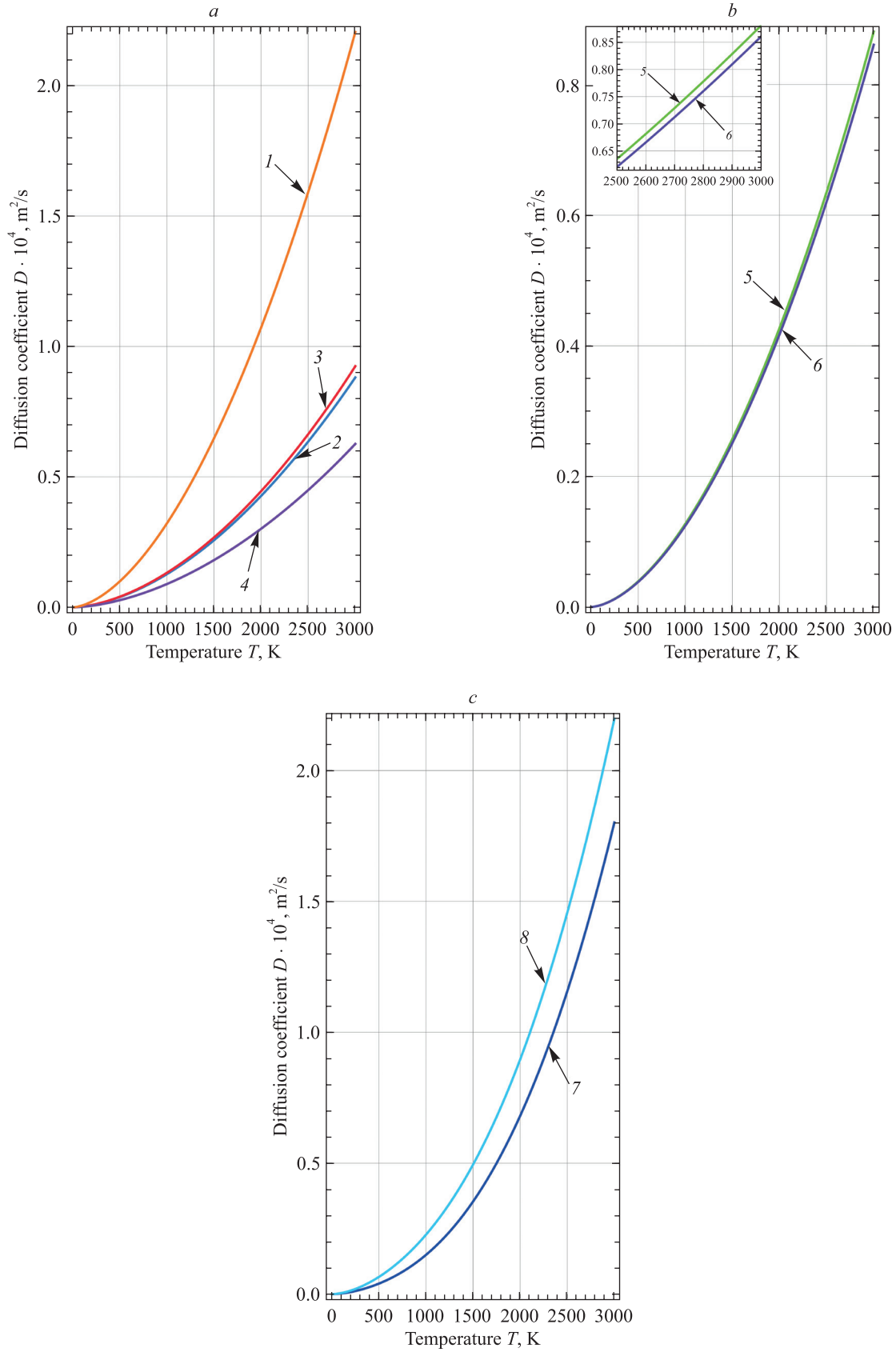
Fig. 7. Predicted diffusion coefficient for the dilute gas media:
illustration *a* demonstrates $^{226}Ra - {}^{19}F$ (*1*), $^{226}Ra - {}^{35}Cl$ (*2*), $^{226}Ra - {}^{79}Br$ (*3*), $^{226}Ra - {}^{127}I$ (*4*);
illustration *b* presents $^{226}Ra - {}^{35}Cl$ (*5*), $^{226}Ra - {}^{37}Cl$ (*6*); illustration *c* shows $^{39}K - {}^{85}Rb$ (*7, 8*)
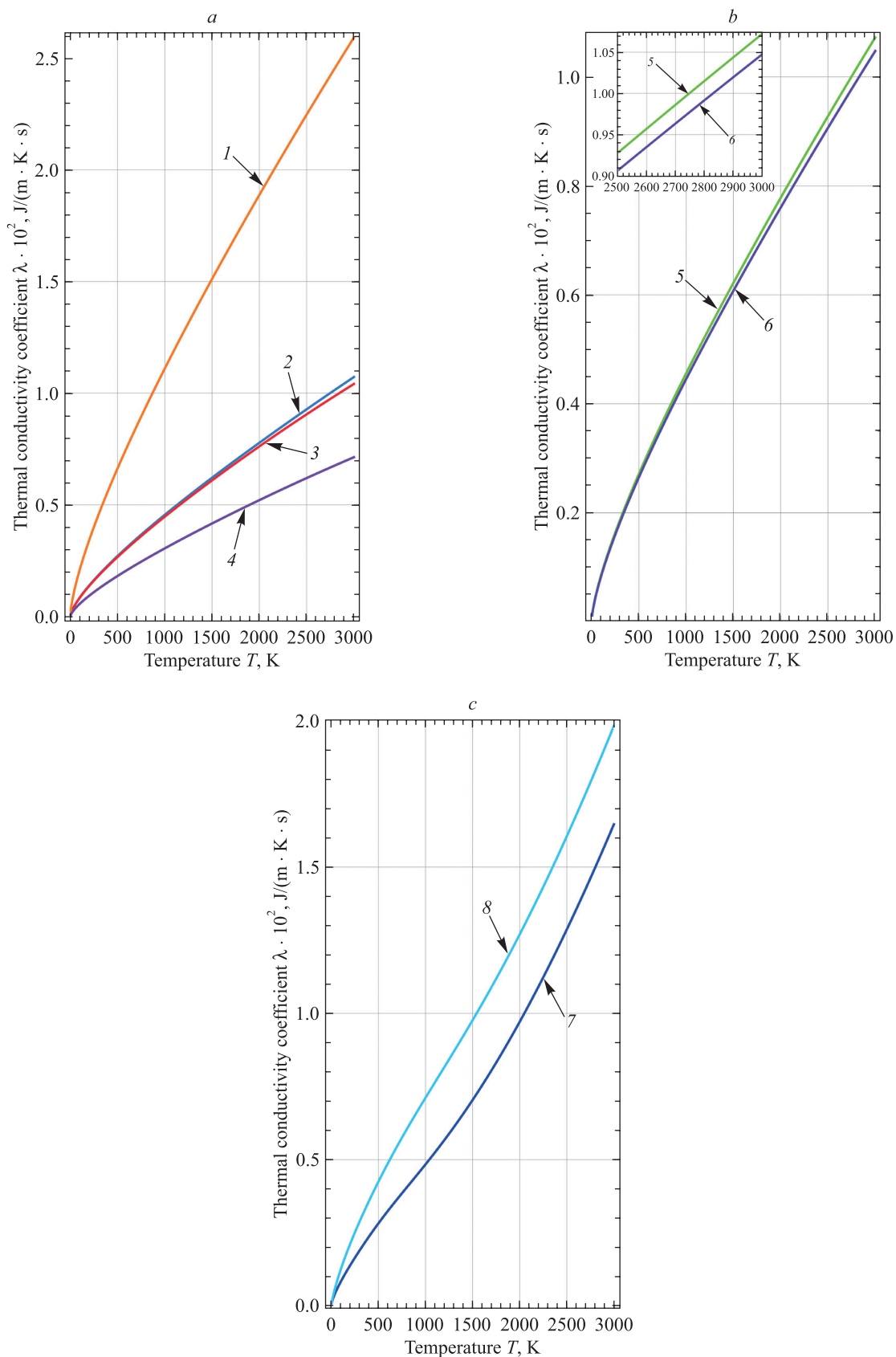
Fig. 8. Predicted thermal conductivity coefficient for the dilute gas media:
illustration *a* demonstrates $^{226}Ra - {}^{19}F$ (*1*), $^{226}Ra - {}^{35}Cl$ (*2*), $^{226}Ra - {}^{79}Br$ (*3*), $^{226}Ra - {}^{127}I$ (*4*);
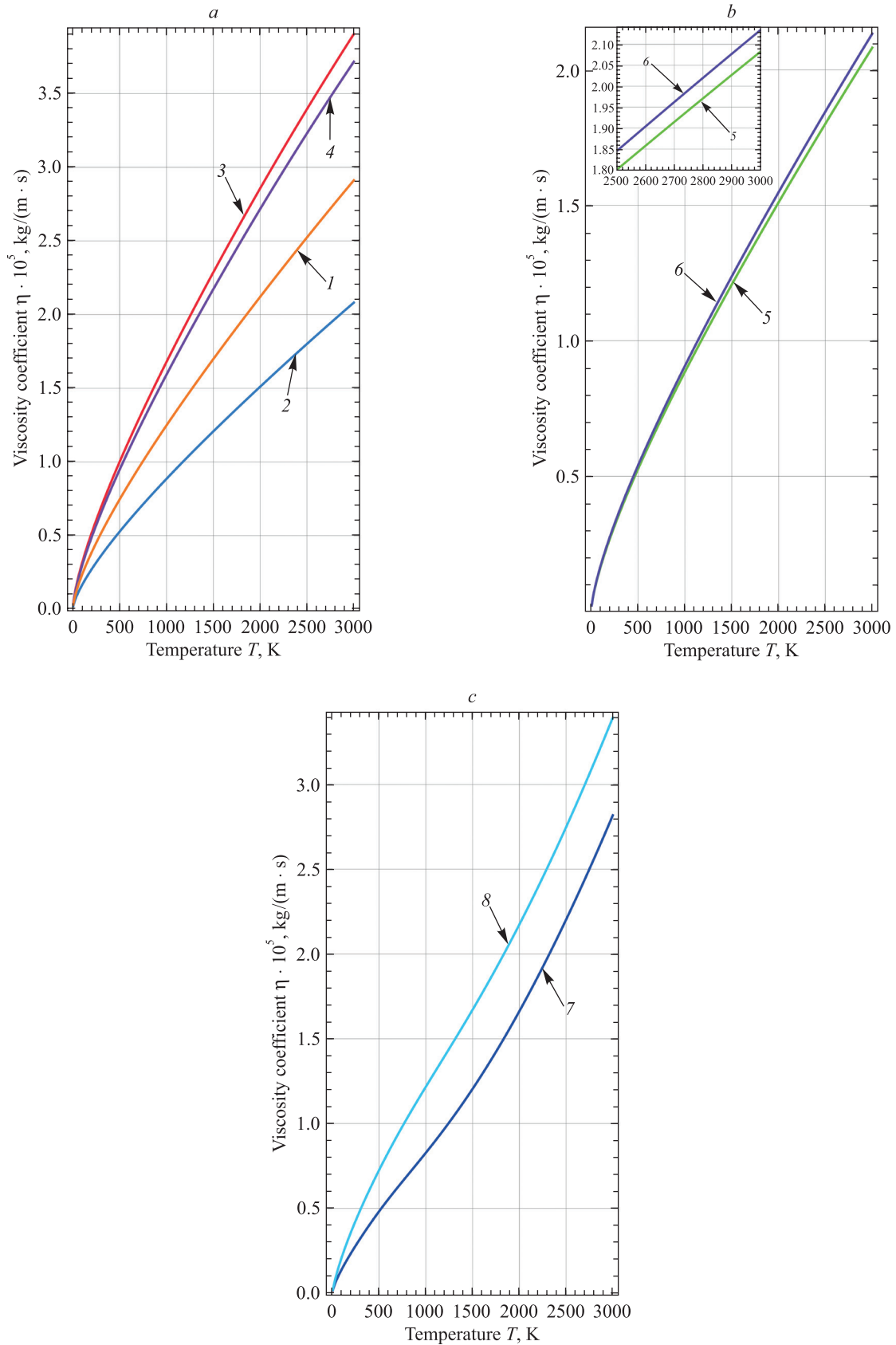illustration *b* presents $^{226}Ra - {}^{35}Cl$ (*5*), $^{226}Ra - {}^{37}Cl$ (*6*); illustration *c* shows $^{39}K - {}^{85}Rb$ (*7, 8*)

Fig. 9. Predicted viscosity coefficient for the dilute gas media:
illustration *a* demonstrates ^{226}Ra – ^{19}F (*1*), ^{226}Ra – ^{35}Cl (*2*), ^{226}Ra – ^{79}Br (*3*), ^{226}Ra – ^{127}I (*4*);
illustration *b* presents ^{226}Ra – ^{35}Cl (*5*), ^{226}Ra – ^{37}Cl (*6*); illustration *c* shows ^{39}K – ^{85}Rb (*7*, *8*)

Conclusions

Based on the classical kinetic theory of gaseous media, a detailed methodology for the calculation of the transport properties using the Morse potential has been developed. The diffusion, thermal conductivity and viscosity coefficients as functions of the translation temperature in the range 5–3000 K for the two-component radium – halogen (F, Cl, Br, I) dilute gas media are calculated for the first time. The influence of an isotope mass on the transport properties is defined. Possible errors introduced by using the model Morse potential function instead of the real potential for the interaction between atoms are estimated. Calculated data can be useful for the planning of the experiments on the direct laser cooling of the monohalides of alkaline earth metals.

References

1. Dulieu O, Gabbanini C. The formation and interactions of cold and ultracold molecules: new challenges for interdisciplinary physics. *Reports on Progress in Physics.* 2009;72(8):086401. DOI: 10.1088/0034-4885/72/8/086401.

2. Tarbutt MR. Laser cooling of molecules. *Contemporary Physics.* 2018;59(4):356–376. DOI: 10.1080/00107514.2018.1576338.

3. Sunaga A, Abe M, Hada M, Das BP. Merits of heavy-heavy diatomic molecules for electron electric-dipole-moment searches. *Physical Review A.* 2019;99(6):062506. DOI: 10.1103/PhysRevA.99.062506.

4. Shuman ES, Barry JF, Glenn DR, DeMille D. Radiative force from optical cycling on a diatomic molecule. *Physical Review Letters.* 2009;103(22):223001. DOI: 10.1103/PhysRevLett.103.223001.

5. Shuman ES, Barry JF, DeMille D. Laser cooling of a diatomic molecule. *Nature.* 2010;467(7317):820–823. DOI: 10.1038/nature09443.

6. Barry JF, McCarron DJ, Norrgard EB, Steinecker MH, DeMille D. Magneto-optical trapping of a diatomic molecule. *Nature.* 2014;512(7514):286–289. DOI: 10.1038/nature13634.

7. Hemmerling B, Chae E, Ravi A, Anderegg L, Drayna GK, Hutzler NR, et al. Laser slowing of CaF molecules to near the capture velocity of a molecular MOT. *Journal of Physics B: Atomic, Molecular and Optical Physics.* 2016;49(17):174001. DOI: 10.1088/0953-4075/49/17/174001.

8. Truppe S, Williams HJ, Hambach M, Caldwell L, Fitch NJ, Hinds EA, et al. Molecules cooled below the Doppler limit. *Nature Physics.* 2017;13(12):1173–1176. DOI: 10.1038/nphys4241.

9. Cheuk LW, Anderegg L, Augenbraun BL, Bao Y, Burchesky S, Ketterle W, et al. Λ-enhanced imaging of molecules in an optical trap. *Physical Review Letters.* 2018;121(8):083201. DOI: 10.1103/PhysRevLett.121.083201.

10. Isaev TA, Hoekstra S, Berger R. Laser-cooled RaF as a promising candidate to measure molecular parity violation. *Physical Review A.* 2010;82(5):052521. DOI: 10.1103/PhysRevA.82.052521.

11. Garcia Ruiz RF, Berger R, Billowes J, Binnersley CL, Bissell ML, Breier AA, et al. Spectroscopy of short-lived radioactive molecules. *Nature.* 2020;581(7809):396–400. DOI: 10.1038/s41586-020-2299-4.

12. Udrescu SM, Brinson AJ, Garcia Ruiz RF, Gaul K, Berger R, Billowes J, et al. Isotope shifts of radium monofluoride molecules. *Physical Review Letters.* 2021;127(3):033001. DOI: 10.1103/PhysRevLett.127.033001.

13. Hirschfelder JO, Curtiss ChF, Bird RB. *Molecular theory of gases and liquids.* New York: Wiley; 1954. 1219 p.

14. Visscher L, Eliav E, Kaldor U. Formulation and implementation of the relativistic Fock-space coupled cluster method for molecules. *Journal of Chemical Physics.* 2011;115(21):9720–9726. DOI: 10.1063/1.1415746.

15. Osika Y, Shundalau M. Fock-space relativistic coupled cluster study on the RaF molecule promising for the laser cooling. *Spectrochimica Acta A: Molecular and Biomolecular Spectroscopy.* 2022;264:120274. DOI: 10.1016/j.saa.2021.120274.

16. Osika Y, Shundalau M. Fock-space relativistic coupled cluster study on the spectroscopic properties of the low-lying states of the radium monobromide RaBr molecule. *Journal of Quantitative Spectroscopy and Radiative Transfer.* 2021;276:107947. DOI: 10.1016/j.jqsrt.2021.107947.

17. Osika Y, Shundalau M, Han Y-C. *Ab initio* study on the spectroscopic and radiative properties of the low-lying states of the radium monoiodide RaI molecule. *Journal of Quantitative Spectroscopy and Radiative Transfer.* Forthcoming 2022.

18. Taylor WL. *Algorithms and FORTRAN programs to calculate classical collision integrals for realistic intermolecular potential* [technical report]. Miamisburg (Ohio): Mound Facility, United States Department of Energy; 1979. 45 p.

19. Colonna G, Laricchiuta A. General numerical algorithm for classical collision integral calculation. *Computer Physics Communications*. 2008;178(11):809–816. DOI: 10.1016/j.cpc.2008.01.039.

20. Isaev TA, Zaitsevskii AV, Oleynichenko A, Eliav E, Breier AA, Giesen TF, et al. *Ab initio* study and assignment of electronic states in molecular RaCl. *Journal of Quantitative Spectroscopy and Radiative Transfer.* 2021;269:107649. DOI: 10.1016/j.jqsrt.2021.107649.

21. Morse PM. Diatomic molecules according to the wave mechanics. II. Vibrational levels. *Physical Review.* 1929;34(1):57–64. DOI: 10.1103/PhysRev.34.57.

22. Pashov A, Docenko O, Tamanis M, Ferber R, Knöckel H, Tiemann E. Coupling of the $X^1\Sigma^+$ and $a^3\Sigma^+$ states of KRb. *Physical Review A.* 2007;76(2):022511. DOI: 10.1103/PhysRevA.76.022511.

23. Shundalau MB, Minko AA. Determination of the optimal energy denominator shift parameter of KRb electronic states in quantum chemical computations using perturbation theory. *Journal of Applied Spectroscopy.* 2016;82(6):901–904. DOI: 1007/s10812-016-0201-9.

24. Shundalau MB, Pitsevich GA, Malevich AE, Hlinisty AV, Minko AA, Ferber R, et al. *Ab initio* multi-reference perturbation theory calculations of the ground and low-lying electronic states of the KRb molecule. *Computational and Theoretical Chemistry.* 2016;1089:35–42. DOI: 10.1016/j.comptc.2016.04.029.

25. Wolfram Research, Inc. *Mathematica. Version 12.2.* Champaign: Wolfram Research, Inc.; 2020.

26. Medvedev AA, Meshkov VV, Stolyarov AV, Heaven MC. *Ab initio* interatomic potentials and transport properties of alkali metal (M = Rb and Cs)-rare gas (Rg = He, Ne, Ar, Kr, and Xe) media. *Physical Chemistry Chemical Physics.* 2018;20:25974–25982. DOI: 10.1039/C8CP04397C.